Origin of indium-[perylene-3,4,9,10-tetracarboxilic dianhydride] interface states studied by outermost surface spectroscopy using metastable atoms

Satoshi Kera,[1,*] Hiroyuki Setoyama,[1] Miki Onoue,[1] Koji K. Okudaira,[1,2,3] Yoshiya Harada,[4] and Nobuo Ueno,[1,2,3]
[1]*Graduate School of Science and Technology, Chiba University, 1-33 Yayoi-cho, Inage-ku, Chiba 263-8522, Japan*
[2]*Center for Frontier Science, Chiba University, 1-33 Yayoi-cho, Inage-ku, Chiba 263-8522, Japan*
[3]*Department of Materials Technology, Faculty of Engineering, Chiba University, 1-33 Yayoi-cho, Inage-ku, Chiba 263-8522, Japan*
[4]*Life Culture Department, Seitoku University, 550 Iwase, Matsudo 271-8555, Japan*
(Received 5 July 2000; published 1 March 2001)

Metastable atom electron spectra (MAES) and ultraviolet photoelectron spectra (UPS) of indium-[perylene-3,4,9,10-tetracarboxilic dianhydride (PTCDA)] system prepared on a MoS_2 single crystal substrate were measured as a function of the In overlayer thickness (Θ_{In}). As observed by a previous UPS experiment, a new band was observed in the original PTCDA energy gap region even by the MAES which detects the outermost surface selectively. The Θ_{In} dependence of this new band intensity measured by the MAES gives a maximum at $\Theta_{In} \sim 1$ Å, suggesting that four In atoms are reacting with one PTCDA molecule at the C═O parts. From the result of the density functional theory (DFT) methods and the enhanced intensity of the new band in the MAES, it was concluded that the new band originates from π state consisting of In $5pz$ AO's.

DOI: 10.1103/PhysRevB.63.115204 PACS number(s): 73.20.−r, 79.60.Jv, 73.61.Ph, 71.15.Ap

I. INTRODUCTION

Organic electroluminescent (EL) devices have attracted a great deal of attention during the past decade.[1] The devices consist of organic layers sandwiched by two metal electrodes, and therefore studies of the interface between metal and organic thin films are of crucial importance in clarifying the device properties. Among these, study of the energy level alignment at the interface, which is important in carrier injection, has been one of the recent main subjects of these systems.[2] There have been many reports of the ultraviolet photoelectron spectroscopy (UPS) on the interfacial electronic structure between metals and organic thin films.[1–6] In addition to the energy level alignment, the overlap of wave functions of the corresponding states is also important for the interfacial property such as carrier transfer through the interface.

The archetypal organic semiconductor perylene-3,4,9,10-tetracarboxylic dianhydride (PTCDA) has gained increasing interest as a material for such organic devices, since the molecules form well ordered multilayers with high stability. The chemical structure of PTCDA molecule is given in Fig. 1. Furthermore, it was reported that thin films of PTCDA provide new band gap states at the interface due to the reaction with substrates or overlayer materials such as GaAs,[4] In, Al, Ti, and Sn.[5] Azuma *et al.*[6] recently studied the origin of the band-gap state of the In/PTCDA system by angle-resolved UPS (ARUPS). They suggested that the appearance of the band-gap state originates from chemical reaction between C═O group sites of the PTCDA molecule and In atoms.[5,6] However, there is only a limited number of work on the origin of the band-gap state, and there seems to be no direct experimental work that gives information on the spatial distribution of the wave function of the gap state. In the present work, we studied the electronic structure of the outermost surface of an In PTCDA system and their wave functions by metastable atom electron spectroscopy (MAES) and UPS.

In MAES, the kinetic energy of electrons ejected from targets T by impact of metastable atoms A^* is analyzed: $T + A^* \rightarrow T^+ + A + e^-$, e^- for energy analysis.[7] MAES selectively detects the outermost surface layer because metastable atoms do not penetrate into inner layers, in contrast to other surface sensitive methods using photons or electrons as the probe. Furthermore, an orbital of the target molecule extending outside the surface interacts more effectively with the metastable atom than inner orbitals, and thus gives a stronger band in MAES.[8] Therefore, the analysis of relative band intensity of MAES provides information on the molecular orientation and the spatial distribution of wave functions at the outermost layer as well.[9]

In this article we describe (i) detailed assignments of MAES features observed for an oriented PTCDA monolayer and In/PTCDA system prepared on a MoS_2 surface with the help of molecular orbital (MO) calculation using density functional theory (DFT) methods; (ii) experimental estimation of the number of reacted In atoms for one PTCDA molecule and reaction sites in the molecule: and (iii) origin of the new band gap state. The enhanced intensity of the band-gap state in the MAES of the oriented In/PTCDA system indicates that the band gap state has a wave function with larger spread than a π wave function of perylene core.

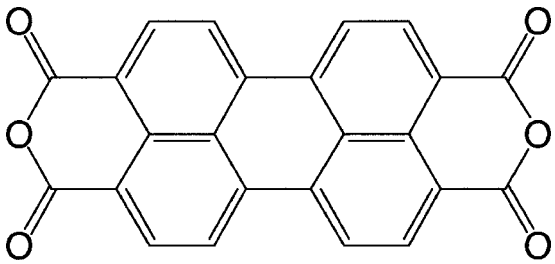

FIG. 1. The structure of perylene-3,4,9,10-tetracarboxylic dianhydride (PTCDA).

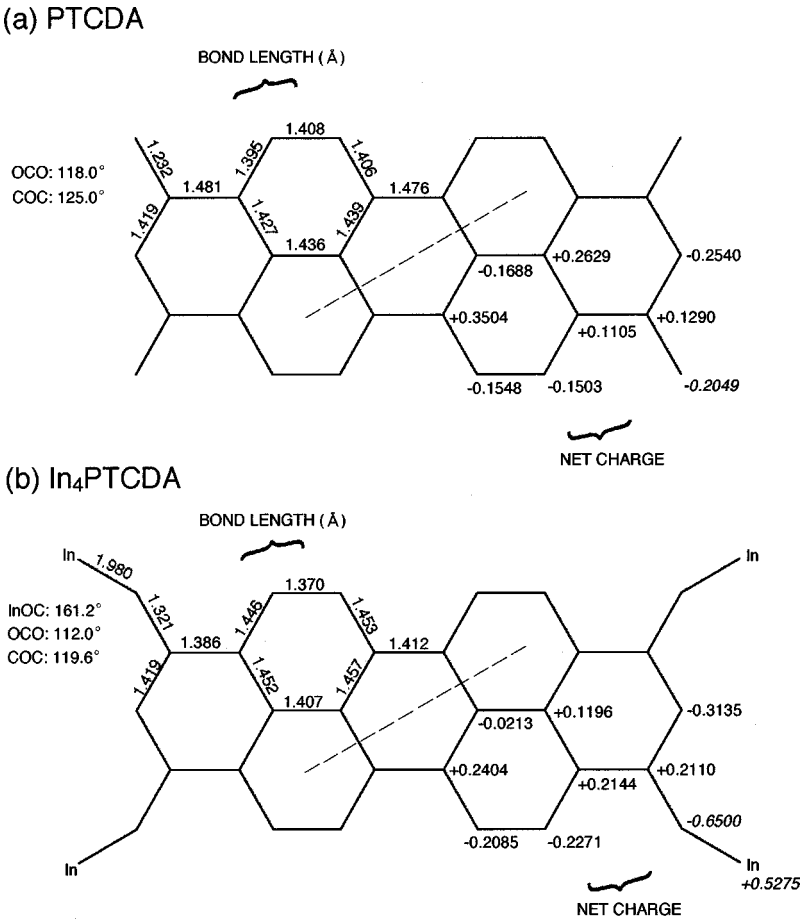

FIG. 2. Optimized molecular geometries and net charges on carbon, oxygen, and indium for pristine PTCDA and a reaction product of In_4PTCDA.

II. EXPERIMENTAL

MAES and UPS were measured by an ultrahigh vacuum (UHV) electron spectrometer with a 180° hemispherical deflection-type analyzer. The apparatus has been reported previously.[10] The metastable atoms of He* (2^3S; 19.82 eV, 2^1S; 20.62 eV) were produced by cold discharge of pure helium gas, giving the high flux beam of the order of $\sim 10^{15}$ atoms s^{-1} sr^{-1}. Details of the He* source was described in Ref. 11. The He*(2^1S) component was quenched by a dc helium lamp (quench lamp) in order to measure the spectra excited by only He*(2^3S). The position of the Fermi level (E_F) was determined from UPS of a thick Au film.

A 2H-MoS_2 crystal[12] was used as the substrate. It was *in situ* cleaved in the preparation chamber and cleaned by heating typically at 200 °C (11 h) and 300 °C (3 h). Cleanliness of the substrate surface was confirmed by measuring MAES just before the deposition of PTCDA. Commercially obtained PTCDA was purified by three cycles of sublimation in an Ar gas stream of ~0.1 Torr, followed by additional two cycles of sublimation in a high vacuum of $\sim 10^{-5}$ Torr. Monolayer films of PTCDA were prepared on the MoS_2 substrate by sublimation in the preparation chamber under UHV. The detail of the molecular orientation of the film is discussed later. Indium was evaporated onto the well-defined flat-lie 1-monolayer film using a resistively heated tungsten filament. The deposited amount of PTCDA and In was monitored with a quartz oscillator calibrated in advance. The deposition rate was about 0.1 *monolayer equivalence* (MLE)/min for PTCDA and ~0.2 Å/min for In. Here, the amount of 1 MLE is defined in such a way that the closely packed molecules, with their molecular planes oriented parallel to the substrate plane, just form a monolayer. One MLE of PTCDA was calibrated by using the occupation area of one PTCDA molecule (138.9 $Å^2$) which was estimated from the unit-cell dimension of the monolayer, $a=13.1$ and $b=21.2$ Å, measured by LEED.[13] The molecular orientation in the 1-MLE film was determined by the method, as described in a previous paper.[9,14–18] Preparation of the well-defined PTCDA monolayer, where the molecules are oriented flat on the substrate surface, is necessary to discuss the origin of the electronic states of the In/PTCDA system, as described later.

The In/PTCDA system was prepared by evaporating In on the flat-oriented PTCDA monolayer. MAES and UPS were measured as a function of the In overlayer thickness (Θ_{In}). The preparation of the films and all MAES and UPS measurements were performed at 100 °C, in order to obtain more complete reaction between PTCDA and In overlayer. For UPS, the binding energies (E_B) are referred to the E_F. For MAES, the E_B are referred to the E_F for a convenient comparison with UPS. In the following, we will not discuss on the vacuum level shift, which is determined from the low kinetic energy cutoff in the spectra, since it is not sufficient for detailed discussion in the present experimental work.

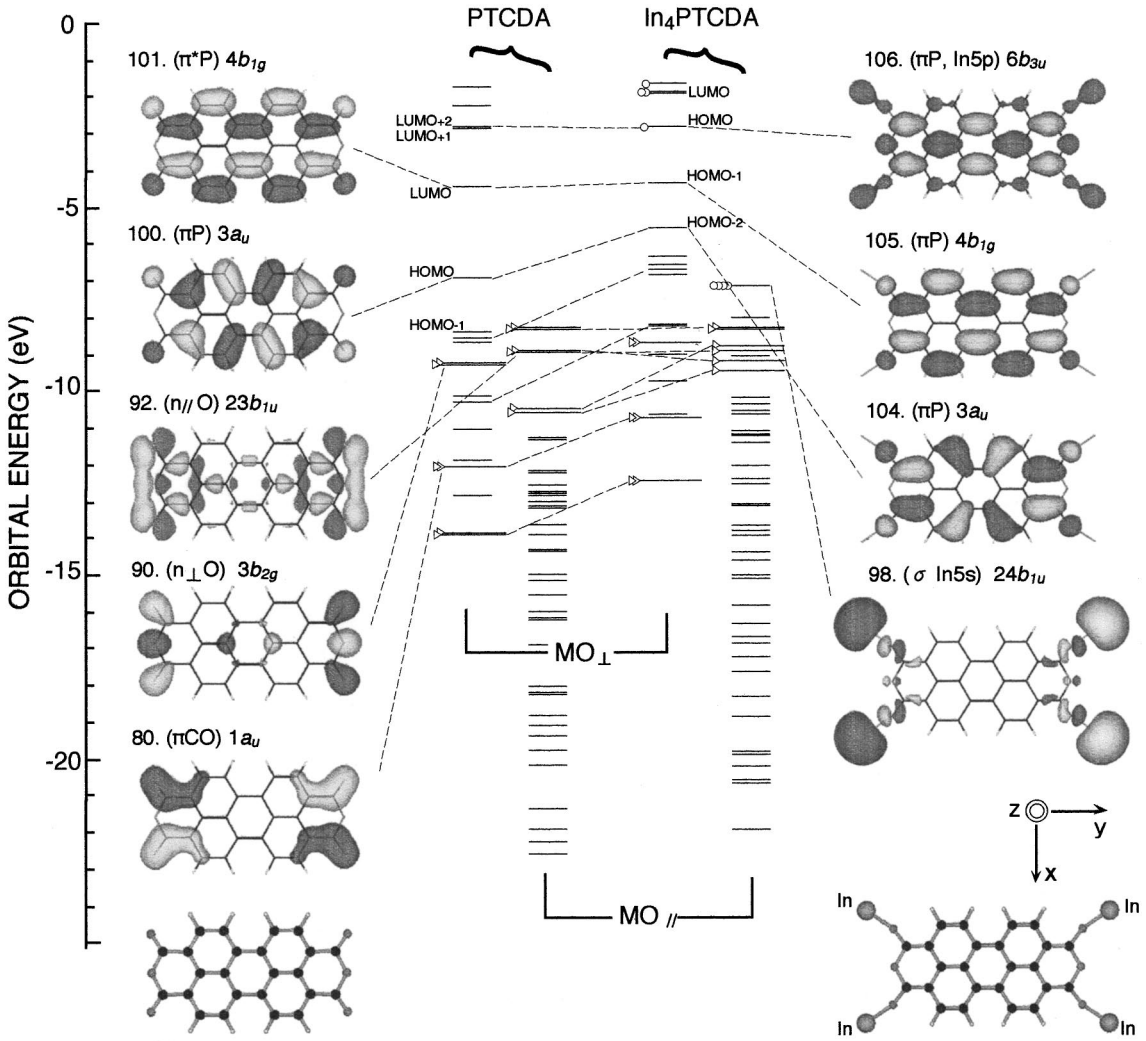

FIG. 3. The correlation among the calculated energy levels obtained by DFT method (B3LYP/LanL2DZ) for PTCDA and In_4PTCDA. The energy levels are divided into two groups, where the left group corresponds to MO's distributed parallel to the molecular plane ($MO_{\parallel}$), oxygen nonbonding ($2p_x$ and $2p_y$) and σ, and the right group displays those distributed perpendicular to the molecular plane ($MO_{\perp}$), π and oxygen nonbonding ($2p_z$). Molecular structure of PTCDA and a model compound of the reaction product, In_4PTCDA, are also shown. In the energy diagrams, MO levels originated from oxygen atoms are shown by slightly longer bars with triangles. Bars labeled with open circles correspond to MO's involving In AO's. Local distributions of the typical MO's of PTCDA (D_{2h}) and In_4PTCDA (D_{2h}) are also shown.

III. RESULTS AND DISCUSSION

A. Molecular orbital calculations

Before showing the observed spectra, we describe results of MO calculations for PTCDA and a model compound of the reaction product, In_4PTCDA, of the In/PTCDA system. The structure of the reaction product was determined as described later. The calculations were performed with the hybrid Hartree-Fock/density functional theory (HF/DFT) method employing the Becke's three-parameter exchange functional[19] combined with the Lee, Yang, and Parr's correlation functional[20] (B3LYP), as implemented in the GAUSSIAN 98[21] program package. In this calculation, the basis set is the Los Alamos National Laboratory set for effective core potentials (ECP) of the double-zeta type (LanL2DZ).[22–24] The DFT approach has been successfully used in earlier descriptions of the interactions of metal atoms with conjugated molecules.[25,26] The geometry of PTCDA (D_{2h} symmetry) and the model compound of the reaction product, In_4PTCDA (D_{2h} symmetry), were fully optimized. In addition, both *ab initio* and semiemprical methods were examined and the calculated results were compared. Among these, we describe here the result of the DFT (B3LYP/LanL2DZ) calculations which yielded the best agreement with the experimental results.

In Fig. 2, we show the optimized molecular geometries of PTCDA and the reaction product In_4PTCDA with the values of the bond lengths, bond angles, and Mulliken atomic charges on carbon, oxygen, and indium atoms (in $|e|$). We find from the net charge of In_4PTCDA that the In atom is calculated to lose about $0.528|e|$; most of this charge is transferred to oxygen atom of C═O part ($0.445|e|$). The perylene core part also receives the large amount of negative

charge $0.538|e|$; total charge around the perylene core is $+0.811$ for PTCDA and $+0.273$ for In_4PTCDA.

Figure 3 shows the correlation between the calculated energy levels of PTCDA and the reaction product In_4PTCDA. MO's distributed perpendicularly to the molecular plane [perpendicular MO ($MO_\perp$)] and those distributed parallely to the molecular plane [parallel MO ($MO_\parallel$)] are shown separately by bars in two columns. Typical orbital patterns are also shown for some selected orbitals. For PTCDA, the calculated energy separation (ΔE) between the highest occupied molecular orbital (HOMO) and the lowest unoccupied molecular orbital (LUMO) is $\Delta E = 6.94 - 4.46 = 2.48$ eV, which is in fair agreement with the experimental value of the lowest electronic transition energy, $\Delta E' = 2.6$ eV, measured by electron energy loss spectroscopy (EELS) for thick PTCDA film.[27] Furthermore, the comparison between the results calculated for PTCDA and the reaction product, In_4PTCDA, leads to the following result. LUMO+2 (see Fig. 3) and LUMO of pristine PTCDA correspond to HOMO and HOMO-1 of In_4PTCDA, which may be related to the electron transfer from In to PTCDA.

B. MAES and UPS features of PTCDA film

We first discuss about the origin of observed spectral features for the pristine PTCDA film. Figure 4 shows the MAES and UPS of 0.2 MLE and 1 MLE PTCDA films prepared on the MoS_2 substrate. The inset spectra show the second derivative of MAES and UPS of the 1-MLE PTCDA with respect to the energy ($-d^2I/dE^2$). As the reference, the UPS of a thicker PTCDA film (20 MLE) on highly oriented pyrolytic graphite (HOPG) substrate are shown after the E_B scale being shifted to the low E_B side by 0.29 eV.[28] ARUPS spectra at two electron take-off angles (θ) measured by Azuma *et al.*[29] and results of the present DFT calculations (B3LYP/LanL2DZ) are also shown. The density of state (DOS) obtained by a Gaussian broadening of the MO levels is shown by solid curve, where MO levels are also shown by separating them into two groups ($MO_\perp$ and $MO_\parallel$). Furthermore, the partial DOS (PDOS) which corresponds to $MO_\perp$ is also shown. Here, all calculated results are compared with experimental results after the calculated E_B scale being shifted to the low E_B side by 4.8 eV.

For the MoS_2 substrate, MAES features do not correspond to those of the UPS, since He* atom is deexcited on the MoS_2 surface predominantly via the resonance ionization (RI)+Auger neutralization (AN) processes.[9] In the UPS, MoS_2 substrate features S_1, S_2, S_3, and S_4 are still clearly visible at the 0.2-MLE PTCDA film [spectrum (c)]. For the 1-MLE PTCDA film [spectrum (d)], the observed valence-band features seem to be also affected slightly by the substrate bands. However, these features correspond well with those of the PTCDA (20 MLE)/HOPG, namely UPS features of the PTCDA (1 MLE)/MoS_2 reflect the valence electronic structure of PTCDA. Moreover, MAES features *A*, *B*, *C'*, *D*, and *E* correspond well to those in the UPS. From this correspondence, we can conclude that the metastable atom is deexcited through Penning ionization (PI) process[9] at the PTCDA film surface.

In the MAES of the 0.2-MLE film [spectrum (a)], the substrate bands S_1' and S_2' were still observed, indicating that the substrate is not fully covered by PTCDA molecules. With increasing thickness of the PTCDA film, intensities of bands S_1' and S_2' were gradually reduced and almost disappeared at 1-MLE deposition [spectrum (b)]. This indicates that the molecules lie flat with their molecular plane oriented parallel to the MoS_2 cleavage plane (flat-lie orientation) and form a uniform monolayer film, since just 1-MLE film of PTCDA shields the MoS_2 substrate for the He* beam.[28] Molecular orientation in the 1-MLE film did not depend on the substrate temperature, which is consistent with results obtained by ARUPS.[29]

In the flat-lie orientation, some MO's are selectively observed in the MAES. Namely, $MO_\perp$ (π,P πCO, and $n_\perp$O) interact more effectively with the metastable atoms, and give stronger bands in the MAES, while $MO_\parallel$ (σ and $n_\parallel$O) scarcely interact with the metastable atoms and are not observed in the MAES. Thus the observed MAES should correspond to the PDOS rather than the DOS. As seen in Fig. 4, the MAES and UPS of the 1-MLE PTCDA have four main valence-bands and these MAES and UPS features are in good agreement with the calculated PDOS and DOS, respectively. From the comparison with calculated results and by considering the characteristic of the MAES, these bands can be assigned as follows. First, in the UPS, band *A* is ascribed to the HOMO band of PTCDA, which consists of a single MO of π character, $3a_u$, distributed over the perylene core (π)P (see Fig. 3). Band *B* is related to some π,P $n_\parallel$O and $n_\perp$O MO's. Here, $n_\parallel$O indicates MO derived from oxygen $2p_x$ and $2p_y$ AO's, which are distributed parallely to the molecular plane (e.g., $23b_{1u}$ in Fig. 3), and $n_\perp$O corresponds to MO derived from oxygen $2p_z$ AO, which is distributed perpendicularly to the molecular plane (for example $3b_{2g}$ in Fig. 3). Band *D* is also related to some πP and $n_\parallel$O. Band *E* is ascribed to πP and πCO which is distributed at C═O and C–O–C parts (e.g., $1a_u$ in Fig. 3), and involves contribution of some σ states that are $MO_\parallel$. These assignments are in good agreement with those of ARUPS bands by using *ab initio* calculation (RHF/STO-6G).[29] An additional band *C* in the ARUPS at $\theta = 70°$ was assigned to four nonbonding orbitals, $n_\parallel$O ($18b_{3g}$,$19b_{2u}$,$24a_g$,$23b_{1u}$) by Azuma *et al.*[29] In the present DFT results, however, energy positions of four $n_\parallel$O MO's are separated from one another and are not located in the energy region of ARUPS band *C*. The disagreement suggests that the MO calculation still needs improvements.

On the other hand, we can assign the observed bands experimentally by comparing MAES, ARUPS, and UPS, since the MAES detects the difference of the spatial distribution of the MO's in the outermost layer, ARUPS features depend on MO characters and the molecular orientation, and UPS is insensitive to these. As described above, in the flat-lie orientation, $MO_\perp$ is selectively observed in MAES. Hence, MAES band *A* is ascribed to πP MO. MAES band *B* is related to four πP MO's. In contrast to the UPS, MAES bands *D* and *E* can be related to only π MO's. A small shoulder *C'*, which was reproducibly observed more

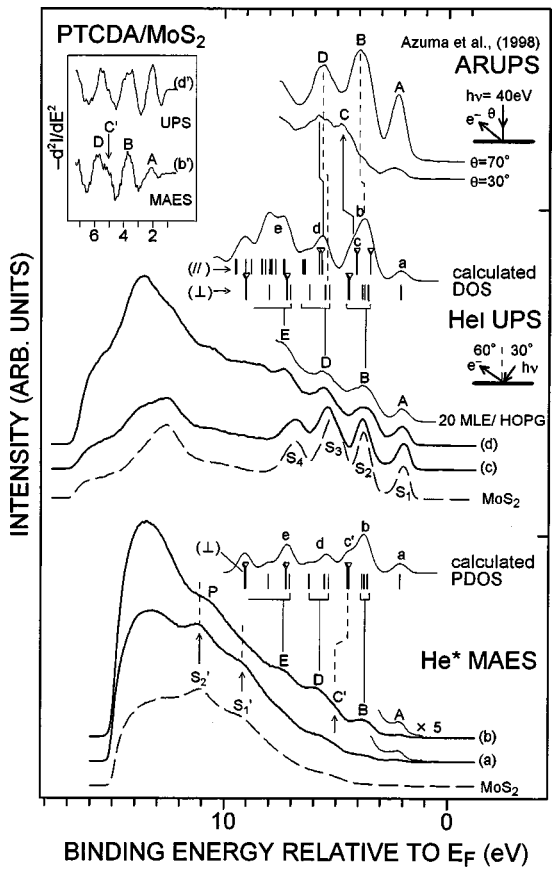

FIG. 4. Comparison of He*(2^3S) MAES, He I UPS of the 0.2 MLE and 1 MLE PTCDA film prepared on a MoS_2 substrate and the calculated results for PTCDA molecule. As a reference, He I UPS of a thicker PTCDA (20 MLE)/HOPG is shown after shifting the energy scale to the low E_B side by 0.29 eV.[28] ARUPS of the PTCDA monolayer film (3 Å) at $\theta = 30°$ and 70° (Ref. 29) are also shown for comparison. In the DOS curve, vertical bars show MO energies obtained by DFT method (B3LYP/LanL2DZ), where energy levels in the upper group correspond to $MO_{\parallel}$ and the lower group to $MO_{\perp}$ (see, also, Fig. 3). Longer bars with triangle indicate states with large contribution of oxygen AO's, namely oxygen nonbonding states ($n_{\parallel}$O and $n_{\perp}$O) or πCO states. The calculated DOS is shown by solid curve, which was obtained by a 0.7 eV Gaussian broadening of MO levels. The PDOS for $MO_{\perp}$ is also shown above MAES spectra. The inset panel shows negative of the second derivative of MAES and UPS of the 1-MLE PTCDA ($-d^2I/dE^2$). For all MAES and UPS measurements and the deposition of the films, samples were kept at 100 °C. The substrate bands in MAES are indicated by S_1' and S_2'. The band P originates from deeperlying band of PTCDA.

strongly in the MAES (see $-d^2I/dE^2$ curve) than in the UPS, corresponds to two $n_{\perp}$O MO's. These results are summarized in Table I, and these band assignments will be used for discussing the origin of electronic states of the In/PTCDA system.

C. Θ_{In} dependencies of MAES and UPS of In/PTCDA system

Figures 5(a) and 5(b) show Θ_{In} dependencies of the MAES and UPS of the In/PTCDA/MoS_2 system, where In

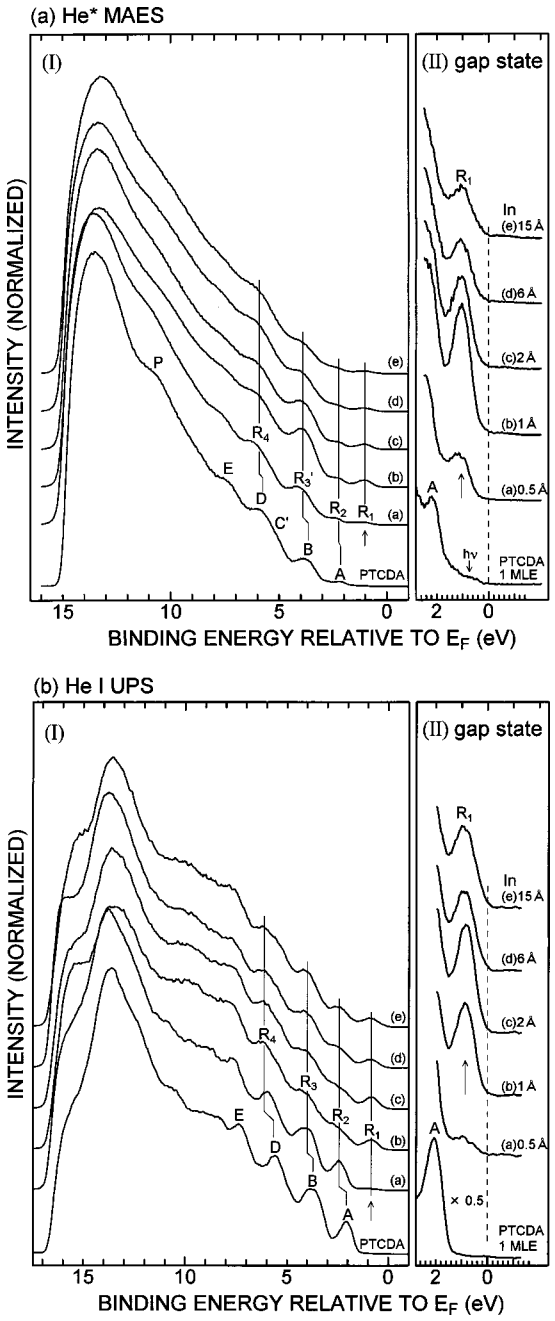

FIG. 5. The dependence of the He*(2^3S)MAES (a) and He I UPS (b) on the thickness of In overlayer (0.5–15 Å) deposited on the oriented 1 MLE PTCDA on MoS_2 held at 100 °C. The full spectra are shown in panel (I). The band-gap region is magnified in panel (II). In the MAES [panel (II)], a weak band ($h\nu$) due to He I, produced by the metastable atom source, is visible.

overlayer was deposited on the oriented 1-MLE PTCDA film. The development of the band-gap state is shown in more detail in panel (II) of Fig. 5. In Fig. 5, the intensity is normalized to the total electron yield. When In overlayer was deposited on the 1-MLE PTCDA film, a new state (band R_1) was observed at ~0.9 eV below E_F in the UPS, namely in the original PTCDA energy gap region as previously observed by UPS[5] and ARUPS.[6] In the MAES, spectral features corresponding to those in the UPS are also observed

TABLE I. MAES and UPS band assignments (MO), energy position from E_F (E_B/eV), and energy relative to band A (ΔE/eV) for PTCDA.

	MAES			UPS		
Band	MO	E_B/eV	ΔE/eV	MO	E_B/eV	ΔE/eV
A	πP	2.1_3	0	πP	2.0_5	0
B	πP	3.6_5	1.5	πP, $n_{\parallel\perp}$O	3.6_6, (3.9)	1.6, (1.9)
C	—	—	—	($n_{\parallel}$O)	4.7[a]	2.7
C'	$n_{\perp}$O	5.0_2	2.9	—	—	—
D	πP	5.7_2	3.6	πP, $n_{\parallel}$O, σ	5.5_0	3.5
E	πP, πCO	7.3 ± 0.1	5.2	πP, πCO, σ	7.2_7	5.2

[a]Reference 29.

(labeled by $R_1 \sim R_4$), indicating that the He* is deexcited by PI process on the In/PTCDA surface as on the 1-MLE PTCDA surface. The detailed assignment of spectral features of the MAES will be described later. The MoS_2 substrate features (S_1' and S_2' in Fig. 4) could not be detected after the In deposition, indicating that the reaction products also shield the substrate surface effectively for the He* beam. Thus, by depositing In on the oriented 1-MLE PTCDA film, it is expected that In-PTCDA reaction products are also oriented nearly flat to the substrate without forming island structure.

In the MAES, the new band R_1 is clearly observed with enough intensity even at $\Theta_{In} \sim 0.5$ Å [see Fig. 5(a)]. With increase in Θ_{In}, the intensity of MAES band R_1 increases up to $\Theta_{In} \sim 1$ Å and then decreases for $\Theta_{In} > 1$ Å. In Fig. 6 the integrated intensities of band R_1 in the MAES and UPS are plotted as a function of Θ_{In} including the data not shown in Fig. 5. It is clearly seen that the band R_1 intensity in the MAES gives a maximum at $\Theta_{In} \sim 1$ Å and decreases for $\Theta_{In} > 1$ Å. It can be understood by considering that the chemical reaction between PTCDA molecule and Indium overlayer is saturated at $\Theta_{In} \sim 1$ Å. For $\Theta_{In} > 1$ Å, Indium islands, which are made up from unreacted In atoms, exist on the reaction products, because we could not detect any MAES features corresponding to atomic In or their small clusters, but clearly observed the formation of In islands by scanning electron microscope (SEM) for a In/PTCDA/MoS_2 system after deposition of thicker In.

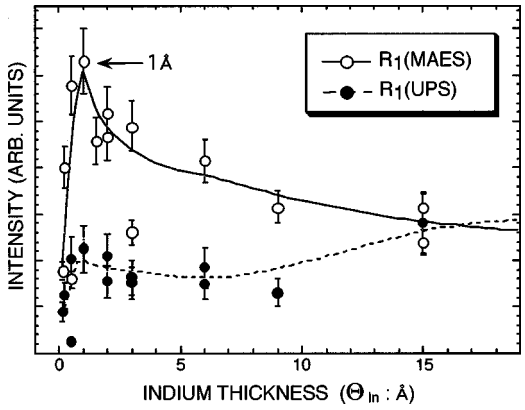

FIG. 6. The In thickness dependence (Θ_{In}) of the band R_1 intensity of MAES (—○—) and UPS (--●--) (see Fig. 5).

In the UPS, on the other hand, the Θ_{In} dependence of the intensity of band R_1 was different from that of the MAES. It showed no prominent peak at $\Theta_{In} = 1$ Å. This difference can be understood by considering the fact that in the UPS, photoelectrons from In islands overlap with band R_1,[28] whereas in the MAES, electrons emitted from the islands give little intensity at this energy region due to the RI+AN process in the deexcitation of He* at the island surface.[28]

We can estimate the number of In atoms that react with one PTCDA molecule from the Θ_{In} value which gives a maximum of R_1 intensity of the MAES. By assuming that sticking coefficients of indium on the surfaces of the quartz oscillator and the sample are the same and that all In atoms react with PTCDA molecule, we obtained that 4.6 In atoms react with one PTCDA molecule at $\Theta_{In} \sim 1$ Å. There exist some unreacted In atoms, and therefore it is expected that four In atoms react with one PTCDA molecule, namely $n_{In}:n_{PTCDA} = 4:1$. Recently, Azuma *et al.* found for the In/PTCDA/MoS_2 system by high-resolution electron energy loss spectroscopy (HREELS) and x-ray photoelectron spectroscopy (XPS) that the interaction between In atoms and PTCDA molecule takes place at C═O parts of PTCDA and not at C–O–C parts.[30] Combining these results, we conclude that In_4PTCDA is produced by the reaction of PTCDA and In contact (see Fig. 2).

D. MAES and UPS features of In_4PTCDA film

In Fig. 7, the calculated electronic structure of the expected reaction product, In_4PTCDA, is compared with the observed MAES and UPS of the In (1 Å)/PTCDA (1 MLE)/MoS_2. The DOS, PDOS, and MO levels of the In_4PTCDA are shown after the binding energy scale being contracted by 0.73 and shifted to the high binding energy side by 1.0 eV, because of the well-known problem of MO calculations to correctly predict the E_B positions. Molecular energy levels for the reaction product, In_4PTCDA, were calculated for optimized ideal plane structure using DFT method (B3LYP/LanL2DZ) as described before. The calculated results agree well with the observed MAES and UPS.

We first note the main difference between the relative band intensities in the MAES and UPS. In the MAES, one can see that the intensity of the gap state R_1 is stronger than that of the second band R_2 (see the $-d^2I/dE^2$ curve and background removed spectrum in Fig. 7). Moreover, the rela-

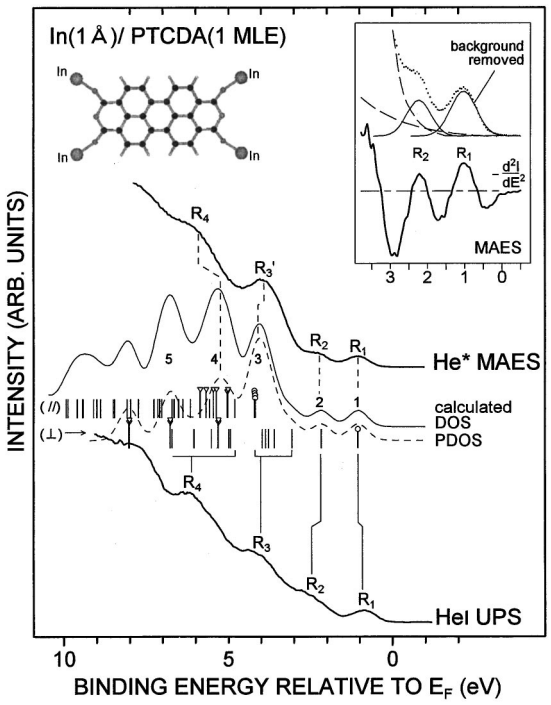

FIG. 7. Comparison of the observed He*(2^3S)MAES and He I UPS of the In(1Å)/PTCDA(1MLE)/MoS_2 and the calculated results for In_4PTCDA. Bars show calculated MO energy levels obtained by DFT method (B3LYP/LanL2DZ). The upper and lower bars, respectively, indicate $MO_{\parallel}$ and $MO_{\perp}$ states, and bars with circles show states with large contribution of In AO's ($5p$,$5s$). Bars with triangles indicate states with contribution of oxygen AO's. The calculated DOS is shown by solid curve. The PDOS, which corresponds to partial DOS for $MO_{\perp}$ and four contracted σ states (marked by circles in $MO_{\parallel}$), is shown by a dashed curve. These DOS's were obtained by 0.7 eV Gaussian broadening of MO's. Negative of the second derivative of the MAES ($-d^2I/dE^2$) and the MAES after background removal is shown in inset, in order to show the enhanced intensity of band R_1 than band R_2. Molecular structure of the reaction product, In_4PTCDA, is also shown (see text).

tive intensity of the third band R_3' in the MAES is especially stronger than the corresponding band R_3 in the UPS. The former result originates from the difference of MO distributions between R_1 and R_2 bands. The latter can be ascribed to the difference of surface sensitivity between MAES and UPS, that is an orbital extending outside the surface interacts more easily with the metastable atom than inner orbitals and gives a stronger band in MAES. The origin of these bands are described later.

The calculated result for the In_4 PTCDA indicates that the top band 1 in the DOS and PDOS is a π state consisting of C $2p_z$, O $2p_z$ and In $5p_z$ wave functions (see Fig. 3, HOMO $6b_{3u}$), and the second band 2 is a π state derived from C $2p_z$ and O $2p_z$ AO's, distributed only in the perylene core (shown by a orbital $4b_{1g}$ in Fig. 3). The third band 3 consists of five π MO's, which involve a π state with MO phase similar to the HOMO state of PTCDA (shown by a orbital $3a_u$ in Fig. 3) and nearly degenerate four σ states with large In $5s$ wave functions (e.g., shown by a orbital $24b_{1u}$ in Fig. 3). The fourth band 4 is related to various MO's such as πP, πCO, $n_{\perp}$O, $n_{\parallel}$O, and σ.

From the fairly-good agreements between the calculated and the observed results, the MAES and UPS bands can finally be assigned as follows. In the UPS, band R_1 is ascribed to πP, involving In $5pz$ AO's, which is in good agreement with those obtained by Azuma *et al.*[6] Band R_2 is related to πP MO. Band R_3 is five πP MO's and σ MO's, involving In $5s$ AO's. Finally, band R_4 is ascribed to various MO's, π, $n_{\perp}$O, $n_{\parallel}$O, and σ states. As described before, on the other hand, the MAES is sensitive to the molecular orientation and detects MO's with large spatial distribution. It is noted that characteristics of the MAES of the In/PTCDA system are (i) the $MO_{\perp}$ (π and $n_{\perp}$O) is mainly observed because the molecules are oriented nearly flat to the substrate and (ii) bands including large In AO give stronger intensities. From these, MAES band R_1 is ascribed to πP, involving In $5p_z$ AO's. Band R_2 is related to πP MO. Band R_3' is πP MO's and σ MO's, involving large In $5s$ AO's. Finally, band R_4 is ascribed to πP, πCO, and $n_{\perp}$O MO's. The E_B values of observed bands in the MAES and UPS and their assignments are summarized in Table II.

In the MAES, band R_1 was observed strongly comparing with band R_2. This is because the wave function for band R_1 (HOMO) consists of large In $5p_z$ AO's and spreads more outside than that for band R_2 (π)P, which consists of only C and O $2p_z$ AO's. Furthermore, the especially strong intensity of the MAES band R_3' in comparison with corresponding band R_3 in the UPS can be due to the effective electron emission from the large In $5s$ derived orbitals by the PI process. The new electronic state, HOMO of In_4PTCDA, has a large wave function that distributes almost normal to

TABLE II. MAES and UPS band assignments (MO), energy position from E_F (E_B/eV), and energy relative to band R_1 (ΔE/eV) for In/PTCDA system.

	MAES			UPS		
Band	MO	E_B/eV	ΔE/eV	MO	E_B/eV	ΔE/eV
R_1	πP (ln $5p_z$)	1.0_5	0	πP(ln $5p_z$)	0.8_6	0
R_2	πP	2.2_6	1.2	πP	2.4 ± 0.2	1.5 ± 0.2
R_3'	πP, σ(ln $5s$)	3.9 ± 0.1	2.9 ± 0.1	—	—	—
R_3	—	—	—	πP, σ(ln $5s$)	4.0 ± 0.2	3.1 ± 0.2
R_4	πP, πCO, $n_{\perp}$O	5.9 ± 0.1	4.9 ± 0.1	πP, πCO, $n_{\parallel\perp}$O, σ	(5.3), 6.1	(4.4), 5.2

the interface plane, and it may play an important role in the charge transfer properties through the interface by bridging the two interface materials.

Finally, we point out that a direct contact of metal and organic films in an UHV would be a new method for synthesizing a new functional compound having small ionization potential.

IV. CONCLUSION

We performed MAES and UPS measurements on In/PTCDA system prepared on a MoS_2 crystal surface. A band is observed in the original PTCDA energy gap region by the MAES as well as by the UPS. From Θ_{In} dependence of MAES, we estimated experimentally that four In atoms react with one PTCDA at C═O parts. Moreover, from the MAES and UPS of the In (1 Å)/PTCDA (1 MLE)/MoS_2 system, origin of the observed MAES and UPS bands are obtained with help from the DFT calculation of the model compound, In_4 PTCDA. The band-gap state of In/PTCDA system originates from the π state involving large In $5p_z$ AO's.

ACKNOWLEDGMENTS

The authors are very grateful to A. Hiratsuka and K. Kimura for their help in measuring MAES and UPS. The present work was partly supported by the Japan Society for the Promotion of Science for Young Scientists and Special Coordination Funds of the Science and Technology Agency of the Japanese Government.

*Author to whom correspondence should be sent; Fax: +81-43-290-3449, Electronic mail: kera.16@xtal.tf.chiba-u.ac.jp

[1] S. R. Forrest, Chem. Rev. **97**, 1793 (1997).
[2] H. Ishii, K. Sugiyama, E. Ito, and K. Seki, Adv. Mater. **11**, 605 (1999).
[3] R. Schlaf, P. G. Schroeder, M. W. Nelson, B. A. Parkinson, P. A. Lee, K. W. Nebesny, and N. R. Armstrong, J. Appl. Phys. **86**, 1499 (1999).
[4] Y. Hirose, W. Chen, R. I. Haskal, S. R. Forrest, and A. Kahn, Appl. Phys. Lett. **64**, 3482 (1994).
[5] Y. Hirose, A. Kahn, V. Aristov, P. Soukiassian, V. Bulovic, and S. R. Forrest, Phys. Rev. B **54**, 13 748 (1996).
[6] Y. Azuma, S. Akatsuka, K. K. Okudaira, Y. Harada, and N. Ueno, J. Appl. Phys. **87**, 766 (2000).
[7] V. Čermák, J. Chem. Phys. **44**, 3781 (1966).
[8] In the following MAES stands for metastable atom electron spectrum as well as for metastable atom electron spectroscopy.
[9] Y. Harada, S. Masuda, and H. Ozaki, Chem. Rev. **97**, 1897 (1997).
[10] T. Munakata, K. Ohno, and Y. Harada, J. Chem. Phys. **72**, 2880 (1980).
[11] S. Yamamoto, S. Masuda, H. Yasufuku, N. Ueno, Y. Harada, T. Ichinokawa, M. Kato, and Y. Sakai, J. Appl. Phys. **82**, 2954 (1997).
[12] L. F. Mattheiss, Phys. Rev. B **8**, 3719 (1973).
[13] A. Schmidt, T. J. Schuerlein, G. E. Collins, and N. R. Armstrong, J. Phys. Chem. **99**, 11 770 (1995).
[14] S. Kera, A. Abduaini, M. Aoki, K. K. Okudaira, N. Ueno, Y. Harada, Y. Shirota, and T. Tsuzuki, J. Electron Spectrosc. Relat. Phenom. **88–91**, 885 (1998).
[15] S. Kera, A. Abduaini, M. Aoki, K. K. Okudaira, N. Ueno, Y. Harada, Y. Shirota, and T. Tsuzuki, Thin Solid Films **327–329**, 278 (1998).
[16] H. Ozaki, M. Kasuga, S. Kera, M. Aoki, H. Tukada, R. Suzuki, N. Ueno, Y. Harada, and S. Masuda, J. Electron Spectrosc. Relat. Phenom. **88–91**, 933 (1998).
[17] T. Pasinzki, M. Aoki, S. Masuda, Y. Harada, Y. Harada, N. Ueno, H. Hoshi, and Y. Maruyama, J. Phys. Chem. **99**, 12 858 (1995).
[18] Y. Harada, H. Hayashi, S. Masuda, T. Fukuda, N. Sato, S. Kato, K. Kobayashi, H. Kuroda, and H. Ozaki, Surf. Sci. **242**, 95 (1991).
[19] A. D. Becke, J. Chem. Phys. **98**, 5648 (1993).
[20] C. Lee, W. Yang, and R. G. Parr, Phys. Rev. B **37**, 785 (1988).
[21] M. J. Frisch, G. W. Trucks, H. B. Schlegel, G. E. Scuseria, M. A. Robb, J. R. Cheeseman, V. G. Zakrzewski, J. A. Montgomery, Jr., R. E. Stratmann, J. C. Burant, S. Dapprich, J. M. Millam, A. D. Daniels, K. N. Kudin, M. C. Strain, O. Farkas, J. Tomasi, V. Barone, M. Cossi, R. Cammi, B. Mennucci, C. Pomelli, C. Adamo, S. Clifford, J. Ochterski, G. A. Petersson, P. Y. Ayala, Q. Cui, K. Morokuma, D. K. Malick, A. D. Rabuck, K. Raghavachari, J. B. Foresman, J. Cioslowski, J. V. Ortiz, B. B. Stefanov, G. Liu, A. Liashenko, P. Piskorz, I. Komaromi, R. Gomperts, R. L. Martin, D. J. Fox, T. Keith, M. A. Al-Laham, C. Y. Peng, A. Nanayakkara, C. Gonzalez, M. Challacombe, P. M. W. Gill, B. Johnson, W. Chen, M. W. Wong, J. L. Andres, C. Gonzalez, M. Head-Gordon, E. S. Replogle, and J. A. Pople (Gaussian, Inc., Pittsburgh, PA, 1998).
[22] P. J. Hay and W. R. Wadt, J. Chem. Phys. **82**, 270 (1985).
[23] W. R. Wadt and P. J. Hay, J. Chem. Phys. **82**, 284 (1985).
[24] P. J. Hay and W. R. Wadt, J. Chem. Phys. **82**, 299 (1985).
[25] C. Fredriksson and S. Staafström, J. Chem. Phys. **101**, 9137 (1994).
[26] C. Fredriksson, R. Lazzaroni, J. L. Brédas, A. Ouhlal, and A. Selmani, J. Chem. Phys. **100**, 9258 (1994).
[27] C. I. Wu, Y. Hirose, H. Sirringhaus, and A. Kahn, Chem. Phys. Lett. **272**, 43 (1997).
[28] S. Kera, Ph.D. thesis, Chiba University, Chiba, 2001.
[29] Y. Azuma, T. Hasebe, T. Miyamae, K. K. Okudaira, Y. Harada, K. Seki, E. Morikawa, V. Saile, and N. Ueno, J. Synchrotron Radiat. **5**, 1044 (1998).
[30] Y. Azuma, Ph.D. thesis, Chiba University, Chiba, 2000.